Biochimica et Biophysica Acta, 595 (1980) 82—95

BBA 78607

I. NOVEL CAPACITATIVE ELECTRODE WITH A WIDE FREQUENCY RANGE FOR MEASUREMENTS OF FLASH-INDUCED CHANGES OF INTERFACE POTENTIAL AT THE OIL-WATER INTERFACE

MECHANICAL CONSTRUCTION AND ELECTRICAL CHARACTERISTICS OF THE ELECTRODE

H.-W. TRISSL

Max-Volmer-Institut für Physikalische Chemie und Molekularbiologie, PC 14 Technische Universität Berlin, Strasse des 17 Juni 135, D-1000 Berlin 12 (Germany)

(Received April 27th, 1979)

Key words: Capacitative electrode; Oil-water interface; Nanosecond measurement; Interface potential change; Photopotential

Summary

The mechanical construction and the electrical properties of a new type of capacitative electrode for the oil-water interface are described. The electrode is designed to detect changes of the interface potential induced by photochemical, photophysical, and photobiological reactions occurring at the interface. The construction is based on capacitative coupling of two aqueous compartments separated by a thin Teflon film. Thereby, the oil-water interface is in horizontal position and the electrode is placed with its planar bottom about 10 μm above the interface. A main feature of the electrode is the transparency to visible light which is achieved by having a clear electrolyte solution in the inner compartment of the capacitative electrode.

The aqueous subphase and the inner electrolyte are connected with Ag|AgCl electrodes to voltage amplifiers. The capacitative electrode is best operated under open circuit conditions. The frequency range experimentally verified is 500 MHz $\gtrsim f_{3dB} \gtrsim$ 0.03 Hz. The sensitivity is mainly determined by the noise of the electronic amplifiers, typical 50—100 μV.

Introduction

The primary processes of photosynthesis, vision, and of the photosynthetic mechanisms of halophilic bacteria take place in membranes of closed vesicles. In all cases the excited pigment molecules initiate electric potential changes at

these membranes. Of special interest are the mechanisms by which light energy is converted into an electrical potential difference. Considerable progress in understanding these processes has been achieved by applying fast-flash spectroscopy methods [1]. The kinetics of the involved reactions could thus be studied with a time resolution between seconds down to picoseconds [2—5]. However, direct electrical measurements of the corresponding electrogenic reactions are scarce. This is mainly due to the smallness of the vesicles which does not allow for microelectrode techniques. In cases where it is possible time resolution is poor and noise is substantial.

One approach to the problem of measuring electrical responses is the spreading of membranes or isolated subunits at a planar apolar-polar interface i.e. the monolayer technique. An advantage of the method is a self-acting orientation of the components in the interfacial layer as well as a large experimental area. This technique has been used for studies of the mitochondrial ATPase [6] and bacteriorhodopsin [7—9]. This paper and the following ones in this series are concerned with the special case of a model system where photoelectrically active material of biological relevance is spread at an oil-water interface. While this communication is devoted to the technical aspects, the subsequent ones deal with photoelectrochemical reactions in photosynthesis, vision, and in bacteriorhodopsin.

Interface potentials at apolar-polar interfaces are commonly measured with special electrodes (for a survey of the matter see Ref. 10). If the apolar phase is sufficiently conductive the electrical potential can be galvanically coupled to metal electrodes. However, when one phase consists of paraffinic oils a capacitative method has to be applied: usually the 'vibrating plate' electrode [10,11]. In the case of air-water interfaces the 'radioactive air gap' electrode is widely used. All three types of electrodes have the disadvantage of a poor time resolution (greater than or approximately equal to 10 ms). In addition, their sensitivity is not sufficient to detect potential changes below 1 mV and, important for flash experiments, it is difficult to illuminate the detection area since all of them are made of metal.

Recently, photoelectric measurements have been published were interfacial layers of visual pigment rhodopsin [12,13] and bacteriorhodopsin [8,9] were asymmetrically attached onto one side of a vertically mounted Teflon film separating two aqueous compartments. The thin Teflon film acts hereby as a coupling capacitor between the electrolyte compartments.

In this paper a new electrode system (capacitative electrode) is introduced which is especially designed for oil-water interfaces in the usual horizontal position. Therefore, the state of the spread material can be controlled by measuring the interfacial tension. The measuring area of the capacitative electrode can be directly illuminated from two opposite sides. The time resolution ranges at least from 10 ns to 10 s.

Materials and Methods

Signals from the electrodes were measured by two electronic detection devices. For slow signals (1): an electrometer amplifier (Keithley, model 602; input characteristics 10^{14} Ω, 20 pF) connected to an electronic storage oscillo-

scope (Nicolet Instrument Corporation, type 'Explorer III'). For fast signals (2): a wide band pulse amplifier with high pulse fidelity (Keithley, model 105; input characteristis 1 MΩ, 10 pF) and a transient recorder (Biomation, model 6500; 2 ns/point). The stored signal from one sweep (this paper) is then transfered to a signal averager (Nicolet Instrument Corporation, model 1170). Finally, the signals from both detection systems were displayed on an *X-Y* recorder.

The test pulses were taken from a function generator (Wavetek, model 162; 30 MHz). The current traces in Fig. 7 were measured with a fast-current amplifier with adjustable bandwidth (Keithley, model 427). Capacitances were measured with a self-built capacitance bridge operating with 100 mV at 1 kHz.

The 12.5 μm transparent Teflon film was purchased from Yellow Springs Instr. Co., whereas the black-stained Kel F was manufactured especially for this purpose by the company 'Pampus' (Willich, F.R.G.).

All Ag|AgCl electrodes were made of sand blasted 1 mm diameter silver wire and coated with current of about 1 mA/cm^2 in 0.1 M HCl. Water was distilled over $KMnO_4$. All organic solvents used were twice distilled in a 0.5 m long glass column.

Clean interfaces were prepared from organic solvent/water mixtures mutually saturated and equilibrated for at least 2 weeks.

Construction. The capacitative electrode is made of polychlorotrifluoroethylene (brand names are: PCTFE, CFE, Voltalef, or Kel F). This material has been chosen because it is resistant against salt water as well as against a variety of organic solvents. Furthermore, the material does not release surface-active agents, is easily cleanable, is mechanically hard, and is a good insulator. Black-stained material is used for protection against stray light.

The technical details of the construction are shown in Fig. 1. The central part of the electrode is a 12.5-μm thick Teflon film which serves to maintain a minimal distance between the electrolyte inside the electrode and the aqueous subphase. The thickness of 12.5 μm reflects a compromise between a good capacitative coupling (= film thickness small) and the avoidance of micropores in thinner Teflon films. The latter cause extensive noise and drifts in the electrical baseline. The film is horizontally clamped between two cylindrical parts which fit into each other as shown in Fig. 1. Sealing occurs at the special conical design at the sharp lower rims of the cylinders. This construction is chosen in order to avoid any grease or glue to obtain tightness. Since the lower rim of the outer cylinder is mechanically stressed the more pliable material Teflon cannot be used for construction. It was observed that tightness is poor and organic solvent enters the cell leading to unstable electrical baselines and excessive noise if this part is made of Teflon.

The two Kel F cylinders sit in an aperture of a stainless steel support where they are positioned and pressed one into the other with four screws. The upper rim of the inner cylinder has a milled groove (cut B-B in Fig. 1) up to which electrolyte is filled. The purpose of this construction is to get a free light path through the electrode and to provide a position where an interconnecting Ag|AgCl rod-shaped electrode is not subjected to illumination. This Ag|AgCl electrode is, in addition, light shielded by a black tube of 4 mm diameter.

The second Ag|AgCl electrode is located in a tube made of black Kel F

which has contact to the aqueous subphase in such a way that the oil and the interface are excluded from the interior of the light-shielding tube. Thereby, the interface remains undisturbed having no contact to metal. The beaker together with the capacitative electrode are enclosed in a Faraday cage.

Results

Principle of operation

A schematic drawing of the electrode system is shown in Fig. 2. At the beginning of an experiment a clean heptane-water interface is prepared as described in Materials and Methods. Then the material under study is spread by injecting it into the interface with a micropipette. A preferential orientation of the molecules with their hydrophobic parts towards the heptane phase and their hydrophilic parts towards the aqueous phase is assumed as indicated in the inset of Fig. 2. The concentration in the interface is determined by measuring the interfacial tension with a carbon black-coated platinum Wilhelmy plate (not shown).

Then the upper part of the electrode system (the 'capacitative electrode') is moved through the heptane phase down to the interface by means of a cog-

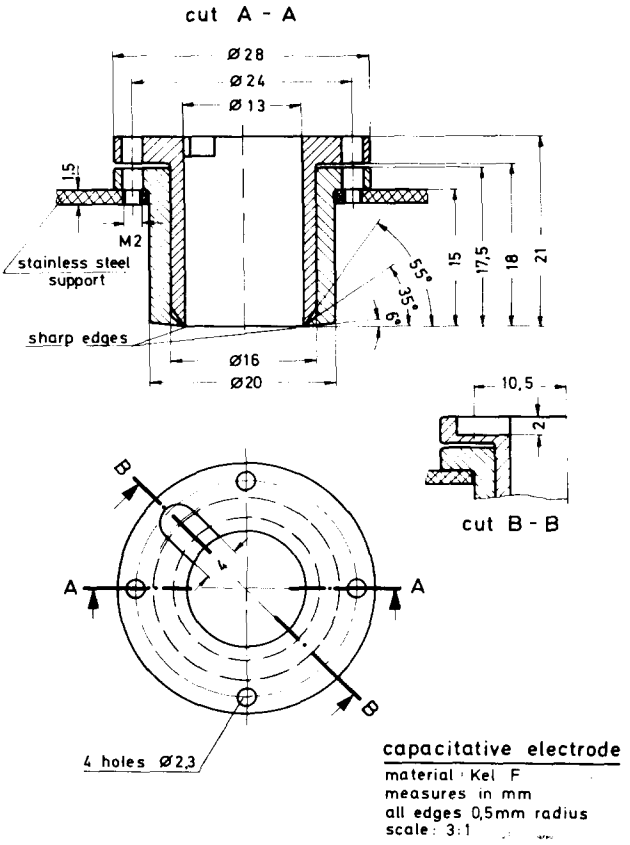

Fig. 1. Workshop drawing of the capacitative electrode. The 'active area' at the bottom is $A = 1.33\ cm^2$.

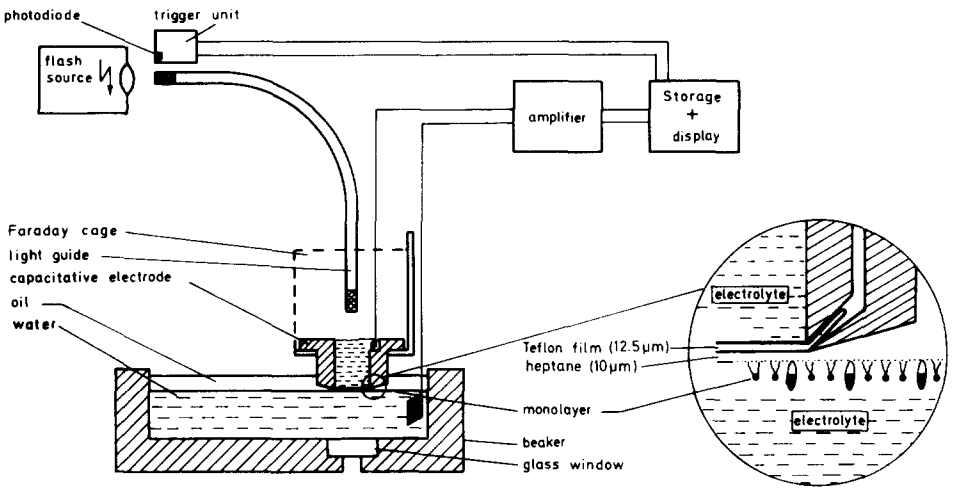

Fig. 2. Schematic representation of the experimental set-up to measure changes of electric potential differences at an oil-water interface with the capacitative electrode.

wheel device. The capacitative electrode consists essentially of a hollow Kel F cylinder the bottom of which is closed with a transparent Teflon film (12.5 μm thickness). The cylinder is filled with electrolyte; in this way transparency and conductivity are provided. In the final stage the Teflon film has a distance of about 10 μm from the interface, so that a high capacitance of the whole system (about 100 pF) is obtained (see inset of Fig. 1).

Illumination of the interface is done via a light guide either from the top through the capacitative electrode or from the bottom through a glass window in the beaker (Fig. 2). Two light-shielded Ag|AgCl electrodes connect the inner electrolyte compartment of the capacitative electrode and the aqueous subphase with a preamplifier. The amplified and/or impendance-converted signals are then stored and displayed with the electronic equipment described in Materials and Methods.

Electrical properties

Determination of capacitance and thickness. In order to bring the capacitative electrode into the working position (i.e. small distance to the oil-water interface) it is slowly lowered through the oil phase by means of a cog-wheel device. During this procedure the oil layer between the electrode bottom and the interface thins out and consequently the capacitance increases. Squeezing out of the oil depends, as experience shows, on the spread material, on the kind of oil, and on the handling of the mechanism to lower the electrode. Examples of continuous recordings of the capacitance versus time are reproduced in Fig. 3. The different curves are either due to different surface-active materials spread at the interface or to clean interfaces of different oils. The absolute values of the capacitance after reaching a steady state lie between 100 pF and 160 pF.

In all cases with oil the steady-state capacitance is lower than the 200 pF

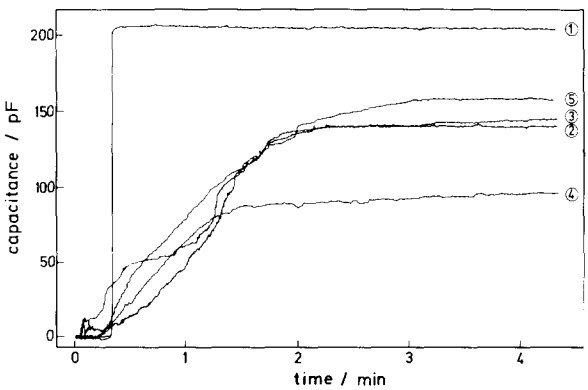

Fig. 3. Time courses of the cpacitance when the capacitative electrode is brought to the interface. The rate of mechanical lowering is approximately the same for all curves. The time courses depend on the rate of lowering as well as on self-acting solvent outflow from the gap between electrode bottom and interface. The aqueous subphase is in all cases 1 M NaCl. Trace 1 results from attaching the capacitative electrode onto a clean water surface without organic solvent. The Teflon film at the bottom of the electrode has not been in contact with oil before. Trace 2 results from a clean *n*-heptane-water interface and trace 3 from a clean *n*-decane-water interface. An interface tension of 50.5 Nm/m (±2%) is measured for the clean interfaces. Trace 4 results from a heptane-water interface with chloroplasts spread and trace 5 from a heptane-water interface with cholesterol spread. The latter two interfacial layers reduce the interfacial tension to about 20 Nm/m.

which are measured when the electrode is put directly onto the aqueous subphase without oil (trace 1 in Fig. 3). The difference results from a residual oil layer directly underneath the Teflon film. The thickness d appertaining to a measured capacitance can be calculated using the formula:

$$d = \frac{\epsilon \cdot \epsilon_0 \cdot A}{C} \tag{1}$$

Taking the area $A = 1.33$ cm^2, a dielectric constant of $\epsilon = 2.1$ for Teflon (ϵ_0 = permittivity of the vacuum) the 200 pF (see Fig. 3, trace 1) correspond with a thickness of 12.5 μm. This is exactly the producers' specification.

The thickness of the remaining oil layer can also be estimated with Eqns. 1 and 2 (see below) and with the known dielectric contant of the oil. It varies between 3 μm and 12 μm depending on the experimental conditions as mentioned above.

Relation between the interface potential change and the measured voltage. An adequate equivalent circuit of the capacitative electrode and the detection device is shown in Fig. 4. The dashed line separates the electrode part from the electronic amplifier part. Since the Teflon film and the oil layer are considered to be perfectly insulating no parallel resistances are drawn. Also the interface is represented by a capacitance only. This will be sufficient for the arguments of this paper, although the equivalent circuit of the interface may be much more complex. The latter has to be discussed separately for any special interface reaction under investigation (for instance see the following paper, Ref. 14).

The active area of the capacitative electrode can be analyzed by considering three capacitors connected in series: The capacitance of the Teflon film C_t, the capacitance of the residual oil layer C_0, and the capacitance of the interfacial

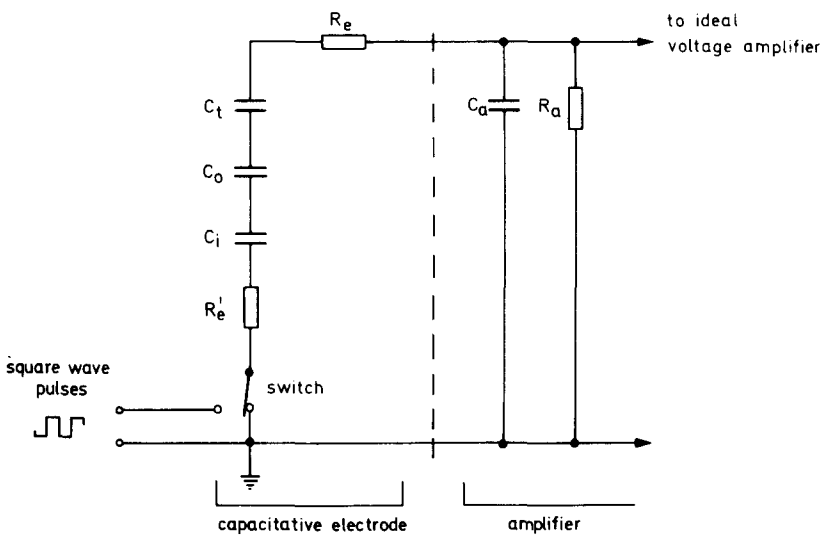

Fig. 4. Equivalent circuit of the capacitative electrode, the voltage amplifier, and the test circuit. For interface measurements the switch is, as drawn, in the closed position. The layer between the inner aqueous compartment of the electrode and the aqueous subphase is split into three separate layers each represented by a capacitor: C_t, Teflon film; C_0, residual oil layer, and C_i, interfacial layer of spread material. The upper and the lower plane of this capacitor stack are connected by electrolyte and Ag|AgCl electrodes with the resistances R_e and R_e' respectively, to the amplifier. At high time resolution R_e and R_e' may become a limiting factor and both should be made small by using large electrode areas and high electrolyte concentration. The voltage amplifier impedance is characterized by the input capacitance (including the leading-in cable) C_a and the input resistance R_a. Optimal measuring conditions are achieved by selecting C_a as small as possible and R_a as large as possible. When the transmission characteristics are to be determined the ground connection is opened and a function generator is introduced. This procedure leaves all other electrical connections unchanged and is considered to be practically equivalent to changes of the charging state of C_i, since $C_i >> (C_0 + C_t)$.

layer C_i. The total capacitance of the active area of the capacitative electrode is given by

$$\frac{1}{C} = \frac{1}{C_t} + \frac{1}{C_0} + \frac{1}{C_i} \approx \frac{1}{C_t} + \frac{1}{C_0} \tag{2}$$

Since the thickness of the interfacial layer can be estimated to be in the order of 100 Å (i.e. $C_i \gg C_t + C_0$) the total capacitance is governed by C_t and C_0 alone.

The detection device cannot discriminate from which one of the subcapacitors a voltage signal originates, but from the lay-out of interface experiments it is obvious that a flash-induced signal originates at C_i, where the photoelectrical active material is spread. In the ideal case this voltage $V_i(t)$ would appear unmodified at the terminals of the capacitor stack. In reality, however, the amplifier input impedance has to be taken into account (right side of Fig. 4). For instance, the amplifier input capacitance C_a (including the leading-in cable) must be charged by the charge generated on C (= capacitor stack) resulting in a loss in amplitude. The actually measured voltage V_a due to this

capacitative voltage divider can be accounted for by a correction formula:

$$V_i(t) = \frac{C + C_a}{C} \cdot V_a(t) \tag{3}$$

In Fig. 5 recorder traces of rectangular pulse trains fed directly into the amplifier are compared with those transmitted through the capacitative electrode. The traces show clearly the smaller amplitudes of the transmitted pulses as compared with the direct recorded ones according to Eqn. 3. A quantitative evaluation of the amplitudes yields a 18 ± 1% voltage loss. The loss predicted from Eqn. 3 is 16% using the separately measured capacitances C = 198 pF and C_a = 35 pF (detection device 1).

Upper and lower limiting frequencies. In this paper two different voltage amplifiers (detection devices 1 and 2) are applied which are selected especially to cover a wide time domain. Besides the bandwidth limitation of the used amplifiers the bandwidth of the complete detecting system is specified by the amplifier input resistance R_a, the amplifier input capacitance C_a, the electrode capacitance C, and the resistances R_e and R'_e (= Ag|AgCl electrode and electrolyte

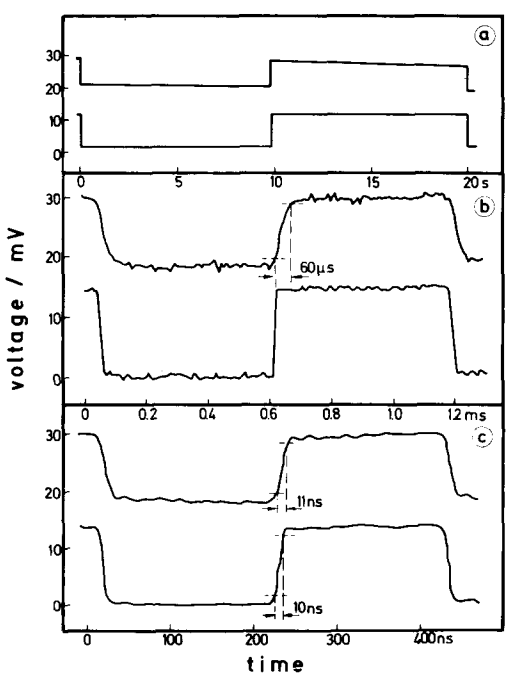

Fig. 5. Examples of the electrical transmission characteristics for three different time ranges. Comparison between square-wave pulses recorded directly with the respective detection devices (lower traces) and those transmitted through the capacitative electrode (upper traces). The inner electrode compartment contains always 3 M NaCl. (a) Transmission at low frequency with detection device 1. (b) High-frequency limitation caused by low NaCl concentration in the subphase (10^{-4} M), measured with detection device 1. The 10—90% rise and fall time of the transmitted pulses is 60 µs (see also Fig. 6). (c) Demonstration of the high-frequency limitation of detection device 2. Aqueous subphase: 3 M NaCl. Note, that all transmitted signals have an undefined offset level (= alternating-current coupling) which can be adjusted arbitrarily. The offset should not exceed the 1 V range because at higher voltages attractive forces compress the capacitor stack so that the oil layer thins out further and C is not any longer constant.

access resistances) the latter depending among other things on the ion concentration.

The lower transmission frequency is determined by the discharge of $(C + C_a)$ through R_a (see Fig. 4). The corresponding time constant τ_l is

$$\tau_l = R_a \cdot (C + C_a) \tag{4}$$

For long-lasting signals it is therefore convenient to use an amplifier with high input resistance (electrometer; detection divice 1). An example of the transmission of rectangular pulses at the long time scale (10 s) with detection device 1 is illustrated in Fig. 5a. This almost ideal transmission characteristic is expected since the exponential decay time calculated from Eqn. 4 is $2 \cdot 10^4$ s. The observed small drift of the transmitted trace is mainly due to the bias current of the galvanically coupled operational amplifier which charges slowly $(C + C_a)$.

The upper transmission frequency of detection device 1 is either given by the limiting frequency of the electrometer (40 kHz) or by the poor conduction of the aqueous subphase when a low ion concentration is chosen. This case is illustrated in Fig. 5b for 10^{-4} M NaCl.

In general, at high frequencies and at low ion concentrations the effect of the access impendance of the electrolyte together with the Ag|AgCl electrodes is crucial: Assuming that the capacitor stack is suddenly charged to the potential V_i, then charge has to flow through the electrodes R_e and R'_e onto C_a until the equilibrium voltage V_a is reached. Thus, the time constant of this charging process describes the fastest rise time possible.

$$\tau_h = (R_e + R'_e) \cdot C_a \tag{5}$$

In order to realize the transmission of fast electrical signals a high electrolyte concentration and a fast voltage amplifier, like that in detection device 2, is required. With $C_a = 20$ pF and an estimate of $R_e = R'_e = 25\ \Omega$ * a rise time of $\tau_h = 1$ ns is calculated. The fastest rise, however, measured with detection device 2 is about 10 ns (see Fig. 5c). This rise time is determined by the components of the detection device: the pulse generator (approx. 8 ns), the pulse amplifier (3 ns), and the transient recorder (3.5 ns). In this example the capacitative electrode itself does not contribute to the maximal time resolution.

When experiments are to be carried out with a subphase of low ion concentration it is essential to know the shortest response time of the capacitative electrode together with the electronic amplifiers. As shown above theoretically (Eqn. 5) the Ag|AgCl electrode-electrolyte resistances may be time limiting. This effect is demonstrated in Fig. 6 with 3 M NaCl in the inner compartment of the capacitative electrode (R_e = constant) and a variable NaCl concentration in the subphase. As seen from the figure the rise time is limited either by salt concentration or by the detection devices.

It should be pointed out that the diagonal straight line in Fig. 6 contains a geometric factor of the electrode areas and of the electrode positions. For

* This is a realistic value for developed Ag|AgCl electrodes (= treated with photographic developer) in concentrated salt solutions and at high frequencies [15].

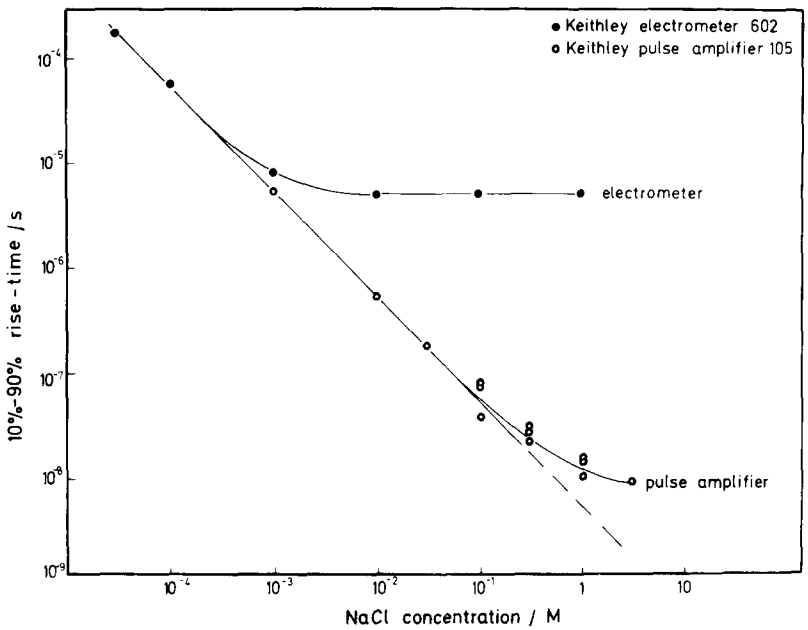

Fig. 6. Rise and fall times of transmitted rectangular pulses as a function of the NaCl concentration in the aqueous subphase. The NaCl concentration in the inner compartment of the capacitative electrode is kept constant at 3 M.

instance, adjusting the Ag|AgCl electrode of the subphase closer to the active area would yield an improved time resolution at all salt concentrations.

Current-voltage relation. The electrical events occurring at the interface might be probed as well by a current-measuring device. This way of detection is applied for instance in Refs. 9, 16 and 17. It will be shown in the following that the current registration contains the same information as the open circuit voltage measurement.

In an ideal current measurement R_a is substituted for a current amplifier with zero input impedance (see Fig. 4). Furthermore, R_e and R'_e are considered to be zero. Then the following equation is derived from the equivalent circuit in order to relate the measured current $i(t)$ and the measured open circuit voltage $V_a(t)$:

$$i(t) = (C + C_a) \cdot \frac{dV_a(t)}{dt} \tag{6}$$

The ideal case is approximated in an experimental set-up where R_e, R'_e, and the current amplifier input resistance R_a are small enough, as to allow that the time constant formed by $(R_e + R'_e + R_a) \cdot C$ is shorter than the shortest signal under investigation.

In order to test the applicability of Eqn. 6 pulses of different shapes are generated in the circuit (at the switch shown in Fig. 4) and measured either with detection device 1 or with an electronic current amplifier. The test in Fig. 7 is performed with sinoidal, triangle, and square-wave waveforms at 1 kHz

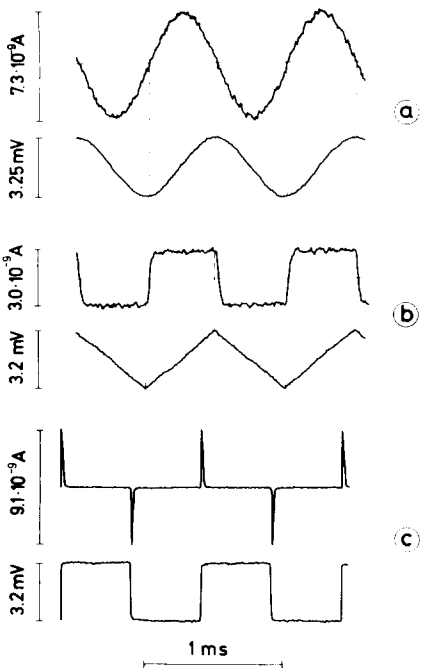

Fig. 7. Current-voltage relation for (a) sinoidal; (b) triangle, and (c) square-wave waveforms at a repetition rate of 1 kHz. The measurement is carried out with the capacitative electrode attached to a 1 M NaCl subphase without using organic solvent. The voltage traces reflect transmitted pulses measured with detection device 1. The current traces are measured by replacing the voltage amplifier by a fast-current amplifier with adjustable bandwidth. The horizontal lines indicate the zero line of the current. The bandwidth of the current amplifier is set to 30 μs.

repetition rate. The current traces are the upper ones and the corresponding voltage traces are underneath.

Since the current and voltage traces should be related in the quantitative manner described by Eqn. 6 one can calculate the capacitance $(C + C_a)$ from the slewing rate of the voltage signals and the measured absolute current. The capacitances calculated in this way are listed in Table I. They agree satisfactorily with the capacitance values independently determined: $C = 201 \pm 3$ pF and $C_a = 34 \pm 1$ pF (compare Figs. 3 and 5).

TABLE I

THE CAPACITANCE $(C + C_a)$ CALCULATED FROM THE TRACES IN FIG. 7 USING EQN. 6

The maximal slope of the voltage and the corresponding current are listed for the traces a and b. Trace c is a special case, since the measured peak current depends exclusively on the rise time setting of the current amplifier. Therefore, the quantitative processing is done by calculating the response time $\Delta t = V \cdot (C + C_a)/i$ from the applied potential step ΔV, 233 pF for $(C + C_a)$, and the measured peak current i. The so calculated 16 μs agree with the producers specification of the current amplifier.

Trace	i (A)	dV/dt ($V \cdot s^{-1}$)	$(C + C_a)$ (pF)
a	$2.3 \cdot 10^{-9}$	9.7	237
b	$1.5 \cdot 10^{-9}$	6.5	231

Whether Eqn. 6 holds also for voltage changes occurring within the oil-water interface will be tested with a photoelectric signal arising from an interfacial layer of the visual pigment rhodopsin (Trissl, H.-W., unpublished results).

Discussion

The capacitative electrode described in this paper covers the extremely wide time domain of more than nine orders of magnitude. This time range is realized by the application of two different electronic detection devices (see Materials and Methods). The detection device 1 which uses an electrometer amplifier covers the range from about 10 μs up to $\gtrsim$ 10 s whereas detection device 2 which uses a wide band pulse amplifier covers the range from about 10 ns to 10 μs. Within these ranges the capacitative electrode itself does not restrict the time resolution. Hence, the connection of the capacitative electrode to faster amplifiers may probably enlarge the measuring range to high frequencies.

The electrical transmission characteristics is determined with test pulses fed into the circuit according to Fig. 4. Although, this procedure is not identical with an interface potential change it is correct within the validity of the equivalent circuit. Whether the operating capacitative electrode is sufficiently described by this equivalent circuit and whether the applied test method is appropriate can only be discussed together with the results of interface reactions (see forthcoming papers of this series).

It is shown in Fig. 5 that the pulse fidelity is excellent over the entire time range studied and that the small voltage loss (= 20%) due to the intrinsic capacitative voltage divider is not frequency dependent. These data are achieved with an open circuit device which gives rise to only small currents in the circuit: Assuming that a potential of 1 mV is generated in 1 ns, this would correspond to a slewing rate of $dV/dt = 10^6$ V/s. The current necessary to charge C_a in this time interval is calculated to $i = C_a \cdot dV/dt = 30$ μA (with C_a = 30 pF). In the case that the signal is detected as a (current voltage clamp it would amount to $i \approx 150$ μA (Eqn. 6). Hence, the currents flowing in the open circuit are five times smaller than those under voltage clamp conditions. In contrast to the 'open circuit' current which depends only on C_a, the current under voltage clamp conditions is proportional to $(C + C_a)$. This means, that in the case of a lipid bilayer membrane, having typically a capacitance C = 10 nF, the internal current would be high as 10 mA.

The open circuit measuring principle has three advantages over a current measurement: (i) the internal currents are smaller; (ii) wide band voltage amplifiers are commercially available whereas a suitable current measuring device for high frequencies is not, and (iii) one obtains the information on the displacement of charges directly when reactions at interfacial layers are studied.

The above arguments also hold for the so-called TVC method introduced by Hong and Mauzerall [16] (TVC = tunable voltage clamp). It is essentially a sophisticated 'potentiostatic method with adjustable access impedance' which can be classified as a current-detecting device. The measuring principle is based on the injection of electronically controlled current, so that the potential at the electrodes remains constant. This is done in order to account for the finite access impedance ('a few hundred ohms', Ref. 16).

In general, high-speed feedback current measuring systems suffer from noise components at higher frequencies exceeding thermal noise [17]. This fact makes the open circuit detection favourable for measurements in the nanosecond range, since this technique can be approached to the limitations of the Johnson noise by commercial amplifiers.

As will be shown experimentally in the following paper for the open circuit system, the effect of a possible access impedance of the interfacial region is negligible. This can be generally understood in terms of the alternating-current resistance $R_c = 1/2\pi f \cdot C_i \approx \tau/C_i$ of an interface capacitance (for instance a Gouy-Chapman capacitance). Although, the ohmic resistance of a difuse ion double layer may be considerable, at high frequencies the large parallel capacitance C_i ($\gtrsim 10\ \mu$ F/cm^2) makes the impedance small.

Since the oil-water interface is in the usual horizontal position and since the interface is not disturbed by the capacitative electrode the interfacial tension can be measured and adjusted by the amount of spread material to defined values. If, for instance, chloroplasts or retinal rod outer segments (vesicular structures) are spread these data can help to decide whether an interfacial layer of vesicles, or a layer of bimolecular or monomolecular structure exists. This was not possible with the geometrical arrangement used in Refs. 8, 9, 12 and 13.

These data concerning the interface can be as well obtained when other types of capacitative electrodes are used [10,11]. However, the capacitative electrode described here has a higher time resolution together with a higher sensitivity as compared with the other electrodes. Furthermore, the detection area can be easily illuminated from two opposite sides, if necessary, with background light and flashes at the same time. This is achieved by connecting galvanically the capacitative part with a transparent electrolyte to Ag|AgCl electrodes.

Although, no absolute values of interface potentials can be measured this capacitative electrode is well suited to detect potential changes in or at oil-water interfaces which arise from light-induced physical, chemical, and biological reactions.

Note added in proof (Received 12th November, 1979)

After this paper had been accepted for publication Huebner reported the construction of an apparatus for recording light-flash-induced membrane voltage transients with 10 ns resolution (Huebner, J.S. (1979) Photochem. Photobiol. 30, 233—241). The basic electronic considerations are very similar to those in this paper. However, time resolution as well as pulse fidelity do not parallel the data reported here due to the use of a different electrometer preamplifier (Burr-Brown, model 3554) by Huebner.

Acknowledgements

The author wishes to thank Prof. H.T. Witt for the general support of this work, Dr. P. Gräber and Prof. W. Junge for critical comments, Mr. A. Aguiñaga (Centro de Investigación del I.P.N., Mexico) for machining the first specimen of the electrode and Mr. H.P. Schröder (Technische Universität Berlin) for

machining further units. This work was financially supported by the Deutsche Forschungsgemeinschaft.

References

1 Rüppel, H. and Witt, H.T. (1969) Methods Enzymol. 16, 316—380
2 Wolff, Ch., Buchwald, H.E., Witt, K. and Witt, H.T. (1969) Z. Naturforsch. 24b, 1038—1041
3 Netzel, T.L., Rentzepis, P.M. and Leigh, J. (1973) Science 182, 238—241
4 Busch, G.E., Applebury, M.L., Lamola, A.A. and Rentzepis, P.M. (1972) Proc. Natl. Acad. Sci. U.S.A. 69, 2802—2806
5 Kaufmann, K.J., Rentzepis, P.M., Stoeckenius, W. and Lewis, A. (1976) Biochem. Biophys. Res. Commun. 68, 1109—1115
6 Yaguzhinsky, L.S., Boguslavsky, L.I., Volkov, A.G. and Rakhmaninova, A.B. (1976) Nature 259, 494—496
7 Hwang, S.-B., Korenbrot, J.I. and Stoeckenius, W. (1977) J. Membrane Biol. 36, 137—158
8 Trissl, H.-W. and Montal, M. (1977) Nature 266, 655—657
9 Hong, F.T. and Montal, M. (1979) Biophys. J. 25, 465—472
10 Davies, J.T. and Rideal, E.K. (1973) Interfacial Phenomena, Academic Press, New York, London
11 Pickard, W.F., Sehgal, K.C. and Jackson, C.M. (1979) Biochim. Biophys. Acta 552, 1—10
12 Trissl, H.-W., Darszon, A. and Montal, M. (1977) Proc. Natl. Acad. Sci. U.S.A. 74, 207—210
13 Trissl, H.-W. (1979) Photochem. Photobiol. 29, 579—588
14 Trissl, H.-W. and Graeber, P. (1980) Biochim. Biophys. Acta 595, 96—108
15 Marmont, G. (1949) J. Cell. Comp. Physiol. 34, 351—382
16 Hong, F.T. and Mauzerall, D. (1974) Proc. Natl. Acad. Sci. U.S.A. 71, 1564—1568
17 Hong, F.T. and Mauzerall, D. (1976) J. Electrochem. Soc. 123, 1317—1324
18 Cath, P.G. and Peabody, A.M. (1971) Anal. Chem. 43, 91A—99A